PHYSICAL REVIEW B **89**, 195203 (2014)

Slow intraband relaxation and localization of photogenerated carriers in $CuIn_{1-x}Ga_xSe_2$ thin films: Evidence for the existence of long-lived high-energy carriers

Makoto Okano,[1] Yutaro Takabayashi,[2] Takeaki Sakurai,[2] Katsuhiro Akimoto,[2]
Hajime Shibata,[3] Shigeru Niki,[3] and Yoshihiko Kanemitsu[1,4,*]
[1]*Institute for Chemical Research, Kyoto University, Uji, Kyoto 611-0011, Japan*
[2]*Institute of Applied Physics, University of Tsukuba, Tsukuba, Ibaraki 305-8573, Japan*
[3]*National Institute of Advanced Industrial Science and Technology (AIST), Tsukuba, Ibaraki 305-8568, Japan*
[4]*Japan Science and Technology, CREST, Uji, Kyoto 611-0011, Japan*
(Received 11 November 2013; revised manuscript received 30 April 2014; published 20 May 2014)

The dynamics of free carriers in polycrystalline $CuIn_{1-x}Ga_xSe_2$ (CIGS) thin films were studied using picosecond time-resolved photoluminescence (PL) and femtosecond transient-absorption (TA) measurements. The PL spectrum and the TA decay component due to the band-to-band recombination of free carriers were observed in the picosecond time region. From excitation-photon-energy-dependent TA measurements, we identified a slow intraband relaxation of free carriers in the CIGS thin films. Collectively, the combination of PL and TA experiments reveal a global feature of energy relaxation and recombination processes of free carriers in the femtosecond to nanosecond time regions.

DOI: 10.1103/PhysRevB.89.195203 PACS number(s): 78.66.Jg, 78.47.D−, 78.47.J−, 78.55.Qr

I. INTRODUCTION

$CuIn_{1-x}Ga_xSe_2$ (CIGS) has attracted considerable interest as a material for highly efficient thin film solar cells because of its advantages such as a high absorption coefficient in the near-infrared and visible spectral regions, controllability of the band-gap energy, and polycrystalline structures that allow easy and large-area fabrications [1–3]. However, in general, polycrystalline semiconductors have complicated optoelectronic properties: They contain grains and defects that serve as carrier traps and recombination centers, because of which these polycrystalline semiconductors exhibit poor luminescence and carrier transport properties as compared to their single-crystal counterparts. Interestingly, the energy conversion efficiency of CIGS solar cells, which exceeds 20%, is the highest among all thin film solar cells despite their polycrystalline structures [2]. The reason for this high efficiency has been a long-standing issue in thin-film-based solar cell research. Considerable efforts from the viewpoint of fundamental physics have been directed toward characterizing grain boundaries (GBs) and defects that determine solar cell performance in CIGS thin films [4–10]. The energy relaxation and recombination dynamics of free photocarriers in polycrystalline CIGS thin films are also crucial factors for the solar cell efficiency.

Transient optical spectroscopy provides essential information on carrier localization and recombination in semiconductors. Over the past two decades, numerous studies have been devoted to the dynamical responses of photoluminescence (PL) and photocurrent in CIGS on the nanosecond time scale [11–18]. The broad PL spectra of CIGS thin films are observed a few hundreds of millielectronvolts below the band-gap energy [19–21]. The PL emission was attributed to radiative recombination of localized carriers in donor and acceptor states below the band edge. A clear observation of radiative band-to-band transition of free carriers has not been reported so far. Therefore, the dynamics of free photocarriers in CIGS thin films have not yet been determined. To gain a deep understanding of highly efficient energy conversion processes in CIGS-based solar cells, it is necessary to determine the dynamics of free carriers in polycrystalline CIGS thin films using ultrafast optical spectroscopy.

In this paper, we report on the energy-relaxation dynamics of free carriers in CIGS thin films, as studied by picosecond time-resolved PL and femtosecond transient-absorption (TA) measurements. These measurements reveal the intraband relaxation and localization times of free carriers and the recombination lifetimes of localized carriers. Even under weak excitation conditions, we observed band-to-band PL and TA signals in the picosecond time region. Photoexcited free carriers show long lifetimes in the nanosecond time region, owing to thermal activation from shallow trap states. We identified an extremely slow intraband relaxation of photocarriers in the CIGS thin films. We suggest that these characteristic features lead to the high solar cell conversion efficiencies of polycrystalline CIGS thin films.

II. EXPERIMENT

The CIGS thin films were grown on soda-lime glass (SLG) substrates by the coevaporation method, using a molecular beam epitaxy technique [3]. The [Cu]/([In]+[Ga]) composition ratio of the CIGS films was approximately 0.93. To conduct TA measurements with a transmission configuration, our CIGS samples with a thickness of 200 nm are an order of magnitude thinner than typical CIGS films. To investigate the effect of the CdS layer on PL and TA measurements, we fabricated CIGS thin films with and without the CdS layer. PL spectra were detected with a liquid-nitrogen-cooled InGaAs diode array through a monochromator, and PL decay dynamics were measured using a near-infrared streak camera. The light source for the PL measurements was a wavelength-tunable Yb:KGW-based femtosecond laser system (300-fs pulse duration and 200-kHz repetition rate). The excitation

*Corresponding author: kanemitu@scl.kyoto-u.ac.jp

photon energy was tuned to 1.75 eV (710 nm) to eliminate the PL from the SLG substrates. In the TA measurements, we used a Ti:sapphire-based femtosecond laser system with two optical parametric amplifiers as the light sources of the pump and probe pulses (150- to 300-fs pulse duration and 1-kHz repetition rate). Optical studies by combining time-resolved PL and TA spectroscopy provide a detailed insight into ultrafast carrier dynamics of solar cell materials [22,23]. All experiments were performed at room temperature.

III. RESULTS AND DISCUSSION

An absorption spectrum of the CIGS/CdS thin film is shown in Fig. 1(a). The inset shows a Tauc plot for direct band-gap semiconductors. By extrapolating the linear function, the band-gap energy E_g of the sample was determined to be ~1.27 eV. The Ga composition (x) of our sample is estimated by the relationship between E_g and x in Ref. [24] to be ~0.48. The absorption spectrum has characteristic structures at around 1.53 and 2.4 eV. By comparison with first-principle band-structure calculations [25–27], the former structure was assigned to the optical transition between the lowest conduction and the split-off valence bands, and the latter structure to the optical absorption of the CdS layer.

Figure 1(b) illustrates the PL spectra at different excitation fluences. The spectra were normalized at the highest emission peak. A few PL peaks appear below and around the band-gap energy. At low excitation fluences below 1.5 μJ/cm^2, only an asymmetric emission peak around 1 eV is observed. In the CIGS films, it is well known that continuous bands are formed by a large number of defects, which act as donors and acceptors [19–21]. Thus, the 1-eV peak can be decomposed into two Gaussian bands reflecting the potential fluctuations due to donors and acceptors [28]: one assigned to the optical transitions between the In_{Cu} defect state (a donor band) and the V_{Cu} defect state (an acceptor band); the other to those between the In_{Cu} and the valence bands in descending order of energy, according to theoretical calculations [29]. This assignment is plausible for our Cu-poor CIGS samples. The energy difference between the V_{Cu} and the valence bands is comparable to the thermal energy at room temperature [29], leading to significant occupation of the valence band, thus light

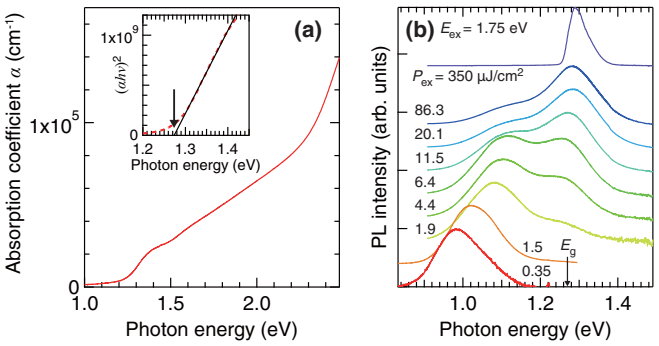

FIG. 1. (Color online) (a) Absorption spectrum of the CIGS thin films at room temperature. The inset shows the Tauc plot in the vicinity of the band edge. (b) Normalized PL spectra of the CIGS thin films for various excitation fluences with excitation at 1.75 eV.

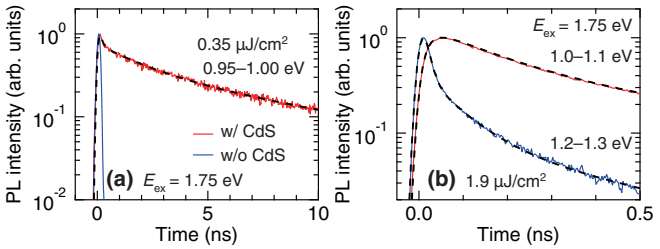

FIG. 2. (Color online) (a) PL decay dynamics in the CIGS thin films with (red curve) and without the CdS layer (blue curve). (b) Blue and red curves correspond to the PL decay dynamics monitored at around 1.05 and 1.25 eV, respectively. In both figures, the black dotted curves represent the fitted curves.

emission due to the transition between the In_{Cu} and the valence bands is observed even under weak photoexcitation.

As the excitation fluence increases above about 2 μJ/cm^2, a new PL peak appears at around 1.27 eV. By comparison with E_g estimated from the absorption spectrum, this peak was assigned to the optical transitions between the conduction band and the V_{Cu} and between the conduction and the valence bands, where the latter corresponds to the band-to-band PL. Band-edge fluctuations due to the Coulomb interaction with acceptors and donors lead to a Gaussian PL shape [28]. As the excitation fluence increases, this PL peak at 1.27 eV shows a slight blueshift due to the state filling, and the contribution of the band-to-band recombination to the PL intensity increases. Finally, we found that under a strong fluence of 350 μJ/cm^2, the band-to-band PL becomes slightly sharper. This is the first observation of radiative band-to-band recombination of free carriers in polycrystalline CIGS films.

To gain deeper insights into the recombination processes of photocarriers, we studied the picosecond PL decay dynamics of the CIGS thin films. Figure 2(a) shows the PL decay curve (red) monitored at photon energies between 0.95 and 1.00 eV in the CIGS thin film with the CdS layer under an excitation fluence of 0.35 μJ/cm^2. Because the PL decay curves show nonexponential behavior, we fitted the curves with triple-exponential functions, $A_1\exp(-t/\tau_1^{PL}) + A_2\exp(-t/\tau_2^{PL}) + A_3\exp(-t/\tau_3^{PL})$; the calculated curves (dotted curves) reproduce the experimental results very well. The three lifetimes obtained are $\tau_1^{PL} \sim 0.15$ ns, $\tau_2^{PL} \sim 2$ ns, and $\tau_3^{PL} \sim 10$ ns. Because the donor-to-acceptor transition is dominant in the PL spectra of CIGS thin films under weak photoexcitation [see Fig. 1(b)], the longest 10-ns PL decay is attributed to the radiative transition from donor to acceptor states. The origins of the other two lifetimes are discussed later by comparison with TA measurements. The PL decay curve (blue) in CIGS films without the CdS layer is also plotted in Fig. 2(a). The PL intensity shows remarkably fast decay, indicating that nonradiative recombination of carriers occurs at oxidized CIGS surfaces [13,18].

We also measured the PL dynamics in the CIGS films with the CdS layer in the region of intermediate excitation fluence, where two PL emission peaks are clearly observed. The PL decay curves monitored at around 1.05 (red) and 1.25 eV (blue) are shown in Fig. 2(b). The PL decay curve of the low-energy peak has a rise time of a few tens of

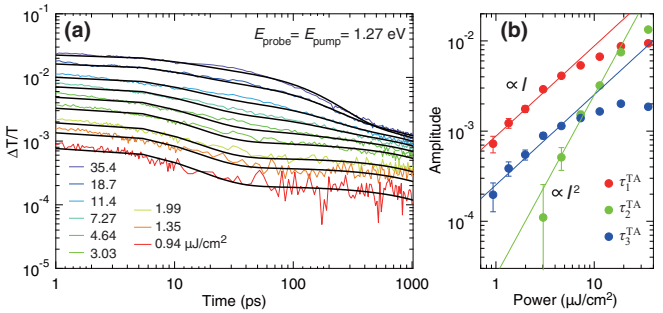

FIG. 3. (Color online) (a) Dependence of TA decay curves for CIGS thin films on the excitation fluence. Pump and probe energies were tuned to E_g. The black curves represent the fitted curves. (b) Amplitudes of the three decay components are plotted as a function of the excitation fluence.

picoseconds. In contrast, the PL decay curve of the high-energy peak has a fast-decay component. We note that the fast decay time of the high-energy PL peak is almost the same as the rise time of the low-energy PL peak. Moreover, the Cu-poor CIGS thin films used here are p-type semiconductors and contain unintentionally doped holes. The PL decay dynamics are determined by localization and recombination of minority carriers, i.e., electrons. Therefore, we conclude that the time constant of a few tens of picoseconds corresponds to the localization of free electrons into the donor states.

To further investigate the energy relaxation and localization dynamics of photocarriers, we studied the TA decay dynamics of the CIGS thin films. Figure 3(a) shows TA decay curves under different excitation fluences ranging from 0.94 to 35.4 μJ/cm^2. The pump and probe pulse photon energies were tuned to E_g. The positive values of $\Delta T/T$ monitored at E_g correspond to photobleaching of the transition between the bottom of the conduction band and the top of the valence band. The positive values for $E_{\rm probe} = E_g$ support our estimation of E_g from the absorption and PL spectra. The TA decay curves at low excitation fluences are well fitted by double exponential functions. The lifetimes are evaluated to be approximately 10 ps ($\tau_1^{\rm TA}$) and 2 ns ($\tau_3^{\rm TA}$). As the excitation fluence increases, a new decay component with a lifetime of about 100 ps ($\tau_2^{\rm TA}$) appears. Electrons are considered to have a predominant impact on the TA signal in the CIGS thin films [30,31], because the effective mass of an electron is smaller than that of a hole in $CuInSe_2$ and $CuGaSe_2$ [26]. Therefore, we conclude that the TA decay dynamics in the CIGS thin films mainly reflect the energy-relaxation and recombination dynamics of photoexcited electrons. Moreover, we note that the fastest decay time $\tau_1^{\rm TA}$ is almost the same as the electron trapping time obtained in the PL dynamics. We assigned $\tau_1^{\rm TA}$ to the relaxation time of free electrons from the conduction band to donor states.

By using the $\tau_1^{\rm TA}$, $\tau_2^{\rm TA}$, and $\tau_3^{\rm TA}$, we performed global fitting of the TA decay curves for the entire excitation fluence range. The obtained amplitudes of these decay components are plotted as a function of the excitation fluence in Fig. 3(b). The uncertainties are small enough to allow discussion of the excitation fluence dependence of the amplitudes. The red, green, and blue symbols correspond to the amplitudes of the $\tau_1^{\rm TA}$, $\tau_2^{\rm TA}$, and $\tau_3^{\rm TA}$ components, respectively. $\tau_1^{\rm TA}$ and $\tau_3^{\rm TA}$ show a linear dependence on the excitation fluence, whereas $\tau_2^{\rm TA}$ shows a quadratic dependence. We found that the band-to-band PL emission becomes dominant as the excitation fluence is increased. Therefore, on the basis of its dependence on the excitation fluence, we conclude that $\tau_2^{\rm TA}$ reflects the recombination of a free electron in the conduction band with a free hole in the valance band [32]. To confirm this assignment, we evaluated the average PL lifetime of the higher emission peak [blue curve in Fig. 2(b)] by averaging the lifetime of the two longer components: $\langle\tau\rangle = \sum_{n=2}^{3} A_n\tau_n / \sum_{n=2}^{3} A_n \sim 120$ ps. The good agreement between $\tau_2^{\rm TA}$ and the average PL lifetime $\langle\tau\rangle$ strongly supports our assignment of the band-to-band transition.

At this point, we would like to comment on the origin of the lifetime $\tau_1^{\rm PL}$, which is also similar to $\tau_2^{\rm TA}$, under weak excitation condition [Fig. 2(a)]. It has been reported that the composition fluctuation occurs in CIGS polycrystalline samples [33]. This suggests that the broad PL peak at 1.0 eV can partly be attributed to the band-to-band recombination with the time constant of approximately 100 ps in the $CuInSe_2$ segment, in which the band-gap energy is approximately 1.0 eV [24]. Since the broad PL emission consists of different carrier recombination processes, we consider that the fitting by a three-exponential function is reliable under weak excitation fluence condition as shown in Fig. 2(a).

The slow-decay components, $\tau_2^{\rm PL}$ and $\tau_3^{\rm TA}$ ($\sim$ a few nanoseconds), are observed under weak photoexcitation in both PL and TA experiments. The TA decay dynamics are mainly determined by the decrease in free carrier density at the band edge when the probe energy, $E_{\rm probe}$, is equal to E_g. In addition, PL experiments [see Fig. 1(b)] show that the radiative transitions between the donor states and the valence band or acceptor states are dominant under weak photoexcitation. Therefore, we can attribute the slow-decay time to the recombination time between electrons trapped in donor states and free holes in the valence band. The long-lived free carriers are mainly ascribed to the thermal excitation from the shallow trap states [29]. The verification of the origin of each decay component was possible by using the combination of PL and TA measurements. Such complementary techniques are helpful to shed light on the carrier dynamics of solar cells.

Next, we conducted TA measurements with different pump photon energies, $E_{\rm pump}$, to investigate the intraband relaxation of photocarriers. Figure 4(a) shows the pump energy dependence of the TA decay dynamics under weak photoexcitation, where $E_{\rm probe} = E_g$. A fast rise during the initial stage appears, except when $E_{\rm pump}$=E_g. As $E_{\rm pump}$ increases, the rise time τ_r, which corresponds to the intraband carrier relaxation through carrier-carrier and carrier-phonon interactions [30,31,34], becomes slower. As explained with Fig. 3(b), the picosecond TA decay dynamics are mainly determined by the electron relaxation from the conduction band to the donor states. Thus, we only considered the electron relaxation process to evaluate the pump energy dependence of the intraband relaxation time. We fitted the TA decay curves by using the following function,

$$I(t) = A\left(e^{\left(-\frac{t}{\tau_d}\right)} - e^{\left(-\frac{t}{\tau_r}\right)}\right).$$

Here, τ_r is the intraband relaxation time from the excited state to the ground state, i.e., the bottom of the conduction

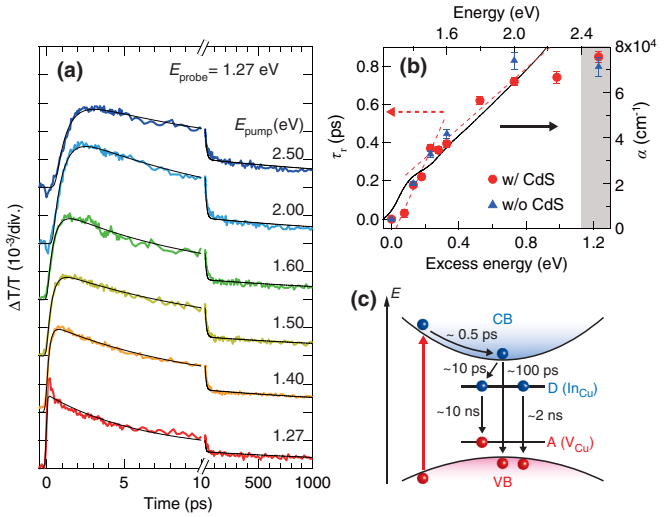

FIG. 4. (Color online) (a) Pump energy dependence of TA decay curves for CIGS thin films under weak excitation conditions. The probe energy was fixed at E_g. The thin black curves represent the fitted curves. (b) Rise times of the TA signals are plotted as a function of the excess energy. The filled circles and triangles correspond to data for CIGS thin films with and without the CdS cap layer, respectively. The black curve plots to the absorption spectrum for reference. The dotted curves represent the fitted curves. (c) A schematic view of carrier relaxation processes in CIGS thin films.

band. A and τ_d are the amplitude and time constant of the exponential function that describes the decay of the electrons at the bottom of the conduction band. Because τ_1^{TA} corresponds to the electron relaxation, the value τ_d obtained through fitting should result in a similar value. Indeed, the fitting of the TA decay curves resulted in $\tau_d \approx \tau_1^{TA}$. To reproduce the TA decay dynamics down to the nanosecond time region, slow relaxation process should be taken into account. Considering slow relaxation with a lifetime of τ_3^{TA}, the TA decay curves are fitted well [Fig. 4(a), black curves]. These facts indicate that τ_1^{TA} and τ_3^{TA}, which are attributed to the relaxation from the bottom of the conduction band, are insensitive to the initial excess energy E_{exc}, which is defined as the energy difference between E_{pump} and E_{probe}, as expected by our model. In Fig. 4(b), the rise times derived from the fitting are plotted as a function of E_{exc}. The intraband relaxation time monotonically increases with E_{exc}. It is noteworthy that no difference is observed between the CIGS samples with and without the CdS cap layer. Therefore, the observed slow intraband relaxation is linked to inherent characteristics of CIGS polycrystalline structure itself.

Moreover, when E_{pump} is larger than 1.5 eV($E_g + 0.2$ eV), the slope of the rise time becomes gentler. Because the split-off valence band lies ~0.2 eV below the top of the valence band [25–27], electrons can be excited from the split-off valence band as well as the lowest valence bands at $E_{pump} > 1.5$ eV. The E_{exc} of the electrons excited from the split-off valence band is much lower than that excited from the two lowest valence bands. The energy loss rate changes at the energy of the split-off valence band, similar to the case of GaAs bulk crystals [30,31,34]. Above $E_{pump} = 2.0$ eV($E_g + 0.7$ eV), the rise time remains almost constant. This is attributed to the effect of intervalley scattering with large wavevector phonons, because the second-lowest conduction-band valley locates approximately 1 eV above the lowest one [25–27]. The relaxation rate is closely linked to the band structure of the CIGS films.

We summarize the carrier relaxation and recombination processes in CIGS thin films in Fig. 4(c). By using a combination of different measurement techniques, we clarified the carrier relaxation times and recombination lifetimes of photocarriers in the CIGS thin films. The most essential point is the slow intraband relaxation of photocarriers with a subpicosecond lifetime. The intraband relaxation rate in CIGS thin films seems to be quite different from that in single crystalline GaAs, a typical direct-gap semiconductor, with an initial intraband relaxation time of a few tens of femtoseconds [30,31]. Thus, we discuss the mechanism of the intrinsic slow intraband relaxation and its impact on solar energy conversion efficiencies in CIGS thin films.

In general, intraband carrier relaxation is governed by two processes: carrier-carrier scattering and carrier-phonon scattering. The carrier-carrier scattering rate depends strongly on the photogenerated carrier density and therefore becomes large under strong excitation fluence conditions. In typical semiconductor such as GaAs, this process plays a dominant role in the initial intraband relaxation on the order of a few tens of femtoseconds [30,31]. However, our experiments showed that the rise time (the intraband relaxation time) under weak excitation fluences is almost the same as that under strong excitation fluences, indicating that the relaxation time does not depend on the carrier density. In our experimental conditions, the carrier-carrier interactions are not dominant in the intraband energy relaxation. The energy relaxation via carrier-phonon interactions determines the rise time of the TA signal, that is, the intraband relaxation.

According to first principle calculations, the second lowest conduction-band valley lies about 1 eV above the band gap energy [25–27]. This suggests that the intervalley carrier-phonon scattering is not an essential intraband relaxation process for sufficient small excitation energies, such as those used in Fig. 4. The intravalley carrier-phonon scattering processes with large-energy optical phonons become dominant only when carriers have large excess energy under high-energy excitation [30,31,35]. Such intravalley carrier-optical-phonon interactions occur on the order of a few hundreds of femtoseconds. The observed slow relaxation in the CIGS samples cannot be explained by the typical intraband energy relaxation processes in single crystalline semiconductors [35].

In CIGS thin films, the composition fluctuation at GBs and the spatial distribution of defect states have been reported [10]. These factors cause the potential to fluctuate near the band edge of the CIGS thin films. We suggest that the potential fluctuations suppress carrier-carrier scattering, because the carriers can be weakly localized at local potential minima, which exist in the valance and conduction bands and are fundamentally different from the localized states existing within the band-gap energy [28]. The photogenerated carriers are located at the local minima in the fluctuated potentials and the slow energy relaxation into the bottom of the conduction band occurs via slow carrier-acoustic-phonon interaction. Moreover, the spatial potential fluctuations are most likely

to further slow down the apparent carrier relaxation, because a carrier must move repeatedly from one local potential minimum to another until it reaches the band edge. Therefore, we believe that the slow intraband relaxation in CIGS thin films is linked to the nature of its polycrystalline structure. The carriers at local potential minima near and above E_g behave as mobile (free) carriers [28], and only these carriers can be considered as "high-energy" carriers. Therefore, the slow intraband relaxation indicates the existence of long-lived high-energy carriers above E_g. The impact of the high-energy carrier lifetime on the performance of inorganic solar cells such as those of CIGS thin films has not yet been clarified. Recent experimental studies have pointed out the importance of high-energy carriers for efficient charge separation in other materials systems for solar cells [36–38]. Our findings imply that long-lived high-energy carriers in CIGS thin films play a crucial role in charge separation and lead to the high performance of CIGS solar cells.

IV. CONCLUSION

In conclusion, we clarified the dynamics of free carriers in CIGS thin films by using time-resolved TA and PL measurements. The band-to-band recombination on the order of subnanoseconds is observed in the PL and TA decay dynamics even under weak excitation fluence conditions. On the basis of the excitation energy dependence of the TA decay dynamics, we revealed that the photogenerated carriers relax slowly into the band edge over the course of several hundreds of femtoseconds and localize in shallow trap states within a few tens of picoseconds. The intrinsic slow carrier intraband relaxation may be of great importance for charge separation in CIGS solar cell applications. Moreover, in spite of the existence of a large number of defect states in polycrystalline films, we found a slow-decay component with a time constant of a few nanoseconds in the TA decay curve owing to the long-lived free carriers. These characteristic dynamical behaviors lead to the high solar conversion efficiency of the CIGS polycrystalline solar cells.

ACKNOWLEDGMENTS

Part of this work was supported by The Sumitomo Electric Industries Group CSR Foundation, KAKENHI (Grant No. 25247052), and JST-CREST.

[1] A. M. Gabor, J. R. Tuttle, D. S. Albin, M. A. Contreras, R. Noufi, and A. M. Hermann, Appl. Phys. Lett. **65**, 198 (1994).
[2] P. Jackson, D. Hariskos, E. Lotter, S. Paetel, R. Wuerz, R. Menner, W. Wischmann, and M. Powalla, Prog. Photovoltaics **19**, 894 (2010).
[3] S. Niki, M. Contreras, I. Repins, M. Powalla, K. Kushiya, S. Ishizuka, and K. Matsubara, Prog. Photovoltaics **18**, 453 (2010).
[4] Y. Yan, C.-S. Jiang, R. Noufi, S.-H. Wei, H. R. Moutinho, and M. M. Al-Jassim, Phys. Rev. Lett. **99**, 235504 (2007).
[5] S. Lany and A. Zunger, Phys. Rev. Lett. **100**, 016401 (2008).
[6] J. Vidal, S. Botti, P. Olsson, J.-F. Guillemoles, and L. Reining, Phys. Rev. Lett. **104**, 056401 (2010).
[7] H. Mönig, Y. Smith, R. Caballero, C. A. Kaufmann, I. Lauermann, M. Ch. Lux-Steiner, and S. Sadewasser, Phys. Rev. Lett. **105**, 116802 (2010).
[8] M. Hafemeister, S. Siebentritt, J. Albert, M. Ch. Lux-Steiner, and S. Sadewasser, Phys. Rev. Lett. **104**, 196602 (2010).
[9] S. S. Schmidt, D. Abou-Ras, S. Sadewasser, W. Yin, C. Feng, and Y. Yan, Phys. Rev. Lett. **109**, 095506 (2012).
[10] D. Abou-Ras, B. Schaffer, M. Schaffer, S. S. Schmidt, R. Caballero, and T. Unold, Phys. Rev. Lett. **108**, 075502 (2012).
[11] B. Ohnesorge, R. Weigand, G. Bacher, A. Forchel, W. Riedl, and F. H. Karg, Appl. Phys. Lett. **73**, 1224 (1998).
[12] S.-C. Chen, Y.-K. Liao, H.-J. Chen, C.-H. Chen, C.-H. Lai, Y.-L. Chueh, H.-C. Kuo, K.-H. Wu, J.-Y. Juang, S.-J. Cheng, T.-P. Hsieh, and T. Kobayashi, Opt. Express **20**, 12675 (2012).
[13] W. K. Metzger, I. L. Repins, and M. A. Contreras, Appl. Phys. Lett. **93**, 022110 (2008); W. K. Metzger, I. L. Repins, M. Romero, P. Dippo, M. Contreras, R. Noufi, and D. Levi, Thin Solid Films **517**, 2360 (2009).
[14] M. Nishitani, T. Negami, N. Kohara, and T. Wada, J. Appl. Phys. **82**, 3572 (1997).
[15] S. Shirakata and T. Nakada, Thin Solid Films **515**, 6151 (2007).
[16] S. Shimakawa, K. Kitani, S. Hayashi, T. Satoh, Y. Hashimoto, Y. Takahashi, and T. Negami, Phys. Status Solidi A **203**, 2630 (2006).
[17] T. Sakurai, K. Taguchi, M. M. Islam, S. Ishizuka, A. Yamada, K. Matsubara, S. Niki, and K. Akimoto, Jpn. J. Appl. Phys. **50**, 05FC01 (2011).
[18] S. Shirakata, H. Ohta, and N. Iwado, Jpn. J. Appl. Phys. **51**, 10NC13 (2012).
[19] I. Dirnstorfer, Mt. Wagner, D. M. Hofmann, M. D. Lampert, F. Karg, and B. K. Meyer, Phys. Status Solidi A **168**, 163 (1998).
[20] J. Krustok, H. Collan, M. Yakushev, and K. Hjelt, Phys. Scr. **T79**, 179 (1999).
[21] M. J. Romero, H. Du, G. Teeter, Y. Yan, and M. M. Al-Jassim, Phys. Rev. B **84**, 165324 (2011).
[22] Y. Yamada and Y. Kanemitsu, Appl. Phys. Lett. **101**, 133907 (2012).
[23] L. Q. Phuong, M. Okano, Y. Yamada, A. Nagaoka, K. Yoshino, and Y. Kanemitsu, Appl. Phys. Lett. **103**, 191902 (2013).
[24] M. I. Alonso, M. Garriga, C. A. Durante Rincon, E. Hernandez, and M. Leon, Appl. Phys. A **74**, 659 (2002).
[25] J. E. Jaffe and A. Zunger, Phys. Rev. B **29**, 1882 (1984).
[26] S. B. Zhang, S.-H. Wei, A. Zunger, and H. Katayama-Yoshida, Phys. Rev. B **57**, 9642 (1998).
[27] S. Siebentritt, M. Igalson, C. Persson, and S. Lany, Prog. Photo. Res. Appl. **18**, 390 (2010).
[28] A. P. Levanyuk and V. V. Osipov, Sov. Phys. Usp. **24**, 187 (1981).
[29] S.-H. Wei, S. B. Zhang, and A. Zunger, App. Phys. Lett. **72**, 3199 (1998).

[30] R. W. Schoenlein, W. Z. Lin, S. D. Brorson, E. P. Ippen, and J. G. Fujimoto, Solid State Electron. **31**, 443 (1988).
[31] W.-Z. Lin, R. W. Schoenlein, J. G. Fujimoto, and E. P. Ippen, IEEE J. Quantum Elec. **24**, 267 (1988).
[32] H. Yasuda and Y. Kanemitsu, Phys. Rev. B **77**, 193202 (2008).
[33] T. Gokmen, O. Gunawan, T. K. Todorov, and D. B. Mitzi, Appl. Phys. Lett. **103**, 103506 (2013).
[34] W. H. Knox, D. S. Chemla, G. Livescu, J. E. Cunningham, and J. E. Henry, Phys. Rev. Lett. **61**, 1290 (1988).
[35] A. Othonos, J. Appl. Phys. **83**, 1789 (1998).
[36] W. A. Tisdale, K. J. Williams, B. A. Timp, D. J. Norris, E. S. Aydil, and X.-Y. Zhu, Science **328**, 1543 (2010).
[37] A. A. Bakulin, A. Rao, V. G. Pavelyev, P. H. M. van Loosdrecht, M. S. Pshenichnikov, D. Niedzialek, J. Cornil, D. Beljonne, and R. H. Friend, Science **335**, 1340 (2012).
[38] A. E. Jailaubekov, A. P. Willard, J. R. Tritsch, W.-L. Chan, N. Sai, R. Gearba, L. G. Kaake, K. J. Williams, K. Leung, P. J. Rossky, and X.-Y. Zhu, Nat. Mater. **12**, 66 (2013).